Computational Investigation of Turbulent Flow Impact on Non-cohesive Soil Erosion near Foundations of Gravity Type Oil Platforms

Alexander Yushkov[1], Igor Nudner[2,3], Konstantin Semenov[2,4], Konstantin Ivanov[1], Nazim Geidarov[1], Sergey Stukolov[1], and Yury Zakharov[1]

[1]Kemerovo State University, Krasnaya, 6, Kemerovo, Russia
[2]23 State Marine Design Institute Branch of "31 State Design Institute of Special Construction", St.-Petersburg, Russia
[3]Baltic State Technical University, St.-Petersburg, Russia
[4]Saint-Petersburg State Polytechnical University, St.-Petersburg, Russia
`zaxarovyn@rambler.ru`

Abstract. The flow turbulence impact on the formation of erosion areas near gravity type oil platforms is studied. The SST (shear-stress transport) turbulence model describing large-scale structures in the internal area and small-scale turbulence in the external area is used for computing turbulent fluid flow. The model grounded on estimation of turbulent behavior of the fluid flow in the bottom flow region where the soil particles transfer is influenced by fluid flow and sea-bed irregularities is applied for estimation of soil erosion. Three sets of numerical studies referred to increase of hydrodynamic values and flow turbulent transition are given.

Keywords: Viscous incompressible fluid, Navier-Stokes equations, non-cohesive soil erosion, three-dimensional flow, turbulence, gravity type oil platforms, numerical and laboratory-based experiments

1 Introduction

The application of gravity type oil platforms at shallow water marine coastal areas is one of the most current means for oil extraction. Processes of sea floor erosion near foundations of such oil platforms and its stability issues are of great interest. In the recent years different investigations of those issues were actively undertaken, by means of laboratory-based and seminatural experiments as well as by means of mathematical simulation [1], [2]. The papers [2], [3] contain results of a great number of experimental and numerical studies of non-cohesive soil erosion near the foundation of the Prirazlomnaya platform, comparison charts of laboratory and simulation experiments, analysis of the impact of different wave conditions of fluid flow on the process of particles shift of seabed material. In those papers the laminar model of fluid flow was applied for numerical evaluation of hydrodynamic quantities. The results of the studies [2] show that when the fluid flow is slow and there are no surface waves, the laminar model provides a good match with laboratory results (up to 10-15% accuracy) on the one

hand, and a significant economy of computational resources, on the other hand. The paper [3] illustrates the waves impact on the structures of soil erosion near the platform foundation. The estimations executed at different wave conditions attest the significant change in the pattern of fluid flow and in the structure of soil erosion when internal flow velocity and wave amplitude are increased. Under such modes the applied in [3] laminar model becomes inoperative. As the results of the former studies show, the increase of the hydrodynamic behavior (that corresponds to small surface waves in a natural experiment) leads to flow laminar-turbulent transition. It is evident that the analysis of such flows demands application of the valid turbulence models. The current paper studies the impact of the developed flow turbulence on the formation of outwashes and inwashes (accretion) near the gravity type oil platforms, both numerically and experimentally. The $k - \omega$, SST (shear-stress transport) turbulence model is applied for estimation of bottom fluid flow velocity that directly constitutes the certain structures of soil erosion. For evaluation of soil erosion we apply the model, which is grounded on the estimation of turbulent properties of fluid flow in the bottom region of the flow. The results of three sets of numerical and experimental studies referred to the increase of the hydrodynamic behavior and flow turbulent transition are given.

2   Flow Model

Variable flow of viscous incompressible fluid with constant properties is described by three-dimensional system of Reynolds-averaged Navier-Stokes in accordance with Boussinesq hypothesis on Newtonian turbulent fluid flow where turbulent viscous stresses are related to average flow properties with the same correspondence as molecular resilient friction is related to velocity field, yet turbulent viscosity needs to be defined instead of 6 components of Reynolds stress symmetric tensor (ν_t):

$$\begin{cases} \frac{\partial U_i}{\partial x_i} = 0, \\ \frac{\partial U_i}{\partial t} + U_j \frac{\partial U_i}{\partial x_j} = -\frac{1}{\rho} \frac{\partial p}{\partial x_i} + \frac{\partial}{\partial x_j} \left((\nu + \nu_t) \frac{\partial U_i}{\partial x_j} \right), \end{cases} \tag{1}$$

where U_i - components of velocity vector, t - time, x_j - Cartesian coordinates, ρ - fluid density, p - pressure, ν - kinematic fluid viscosity, ν_t - turbulent eddy viscosity estimated on the ground of the applied turbulence model.

The present paper applies $k - \omega$, SST (shear-stress transport) turbulence model [4], where k - turbulent kinetic energy, ω - specific dissipation rates referred to isotropic dissipation as follows as: $\varepsilon = \beta^* k \omega$, where $\beta^* = 0.09$.

The classic $k - \omega$ model [5] has issues while calculating stream flows due to extreme sensitivity to boundary conditions in the external flow. The model $k - \omega$, SST, suggested by Menter, eliminates the said imperfection and combines the benefits of $k - \omega$ and $k - \varepsilon$ turbulence models. Menters model applies the modified $k - \omega$ model designed for description of large-scale structures in the internal area, and in the external area - $k - \varepsilon$, aimed to solution of small-scale

turbulence. In Menters model, the model $k - \varepsilon$ is re-formulated in terms k and ω, and a special transition function is added in the received equations in order to transfer from one model to another. The model $k - \omega$, SST is grounded on two equations, the one is for turbulent kinetic energy and the second is for specific dissipation:

$$\frac{\partial k}{\partial t} + U_j \frac{\partial k}{\partial x_j} = P_k - \beta^* k\omega + \frac{\partial}{\partial x_j}\left((\nu + \sigma_k \nu_t) \frac{\partial k}{\partial x_j} \right), \qquad (2)$$

$$\begin{aligned} \frac{\partial \omega}{\partial t} + U_j \frac{\partial \omega}{\partial x_j} &= \frac{\alpha}{\rho \nu_t} \tau_{ij} \frac{\partial U_i}{\partial x_j} - \beta \omega^2 + \frac{\partial}{\partial x_j}\left((\nu + \sigma_\omega \nu_t) \frac{\partial \omega}{\partial x_j} \right) + \\ &+ 2\left(1 - F_1\right)\sigma_{\omega 2} \frac{1}{\omega} \frac{\partial k}{\partial x_i} \frac{\partial \omega}{\partial x_i}, \end{aligned} \qquad (3)$$

where

$$\tau_{ij} = \rho \nu_t \left(2S_{ij} - \frac{2}{3}\frac{\partial U_k}{\partial x_k}\delta_{ij} \right) - \frac{2}{3}\rho k\delta_{ij},$$

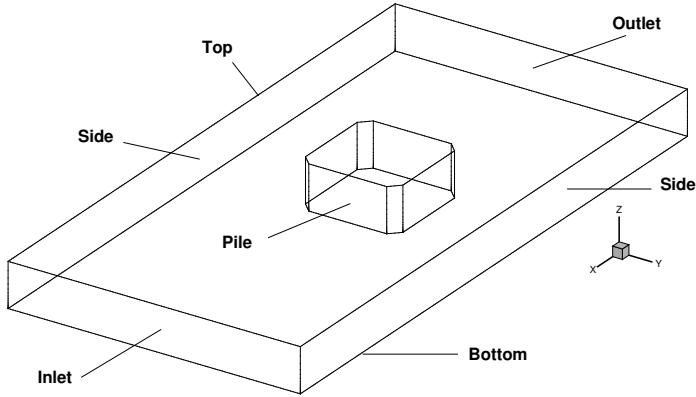$$S_{ij} = \frac{1}{2}\left(\frac{\partial U_i}{\partial x_j} + \frac{\partial U_j}{\partial x_i} \right).$$

Fig. 1. Flow region boundaries

The transition function F_1 is determined as follows as:

$$F_1 = \tanh\left[\left(\min\left[\max\left(\frac{\sqrt{k}}{\beta^* \omega y}, \frac{500\nu}{y^2 \omega} \right), \frac{4\rho \sigma_{\omega 2} k}{CD_{k\omega} y^2} \right] \right)^4 \right], \qquad (4)$$

where $CD_{k\omega} = \max\left(2\rho \sigma_{\omega 2}\frac{1}{\omega}\frac{\partial k}{\partial x_i}\frac{\partial \omega}{\partial x_i}, 10^{-10} \right)$, y - distance to the surface. Turbulent eddy viscosity is determined by the following formula:

$$\nu_t = \frac{a_1 k}{\max\left(a_1 \omega, SF_2 \right)}, \qquad (5)$$

where

$$S = \sqrt{2S_{ij}S_{ij}},$$

$$F_2 = \tanh\left[\left[\max\left(\frac{2\sqrt{k}}{\beta^*\omega y}, \frac{500\nu}{y^2\omega}\right)\right]^2\right],$$

$$P_k = \min\left(\rho\nu_t\frac{\partial U_i}{\partial x_j}\left(\frac{\partial U_i}{\partial x_j} + \frac{\partial U_j}{\partial x_i}\right), 10\beta^*\rho k\omega\right),$$

.

$$\sigma_k = F_1\sigma_{k1} + (1 - F_1)\sigma_{k2},$$
$$\sigma_\omega = F_1\sigma_{\omega1} + (1 - F_1)\sigma_{\omega2},$$
$$\alpha = F_1\alpha_1 + (1 - F_1)\alpha_2,$$
$$\beta = F_1\beta_1 + (1 - F_1)\beta_2.$$

The models invariables are: $\alpha_1 = \frac{5}{9}, \alpha_2 = 0.44, \beta_1 = \frac{3}{40}, \beta_2 = 0.0828, \sigma_{k1} = 0.85, \sigma_{k2} = 1, \sigma_{\omega1} = 0.5, \sigma_{\omega2} = 0.856.$

For completion of the objective it is necessary to postulate the boundary conditions for the components of velocity vector U_i, pressure p, turbulent kinetic energy k and specific dissipation ω.

In the inlet (Fig. 1): $U_1 = u_0, U_2 = 0, U_3 = 0, \frac{\partial P}{\partial n} = 0, k = k_0, \omega = \omega_0$, where u_0, k_0, ω_0 are selected on the basis of comparison of velocity profile at the entrance with the experimental data. In the outlet: $\frac{\partial U_i}{\partial n} = 0, P = 0, \frac{\partial k}{\partial n} = 0, \frac{\partial \omega}{\partial n} = 0$, On the top surface: $\frac{\partial}{\partial n} = 0$ for all variables. On the side surface, pile and bottom: $U_i = 0, \frac{\partial P}{\partial n} = 0, k = 0, \omega = 10\frac{6\nu}{\beta y^2}$, where $\beta = 0.075$, and y - distance from the surface to the center of the closest mesh.

3 Scour Model

The paper [6] applies the model of soil erosion [7], where computations are based on the values of shear stress on the bottom surface. Here bottom is represented by a certain surface divided into meshes by the grid. At first, the vector of soil particles transport through each mesh is estimated, and then the height of the bottom is determined on the ground of mass balance equation.

Within the frames of the present numerical model, particle motion is influenced by the impact of fluid flow and irregularities in bottom surface. For each design moment, bottom shear stress is estimated at first, and then the calculation of the particle motion on the bottom surface is done and mass balance equation is solved.

Two-dimensional coordinate system (x_1, x_2) is implemented for the bottom surface. In order to estimate the stress vector $\bar{\tau}_b$ it is necessary to find the product of stress tensor T and surface normal $\bar{n}$, and then the received vector is projected to the bottom surface.

To determine the vector component $\bar{\tau}_b$ it is necessary to know the value of turbulent eddy viscosity ν_t. In case of application of the laminar model of the

flow while computing velocity field, this parameter was assigned manually to be equal to the average value ν_t at the turbulent flow mode with analogous parameters (size of order $10^{-5} - 10^{-4}$).

After computing the component of shear stress vector, we determine vector $\bar{q} = (q_1, q_2)$ of bottom seabed material in unit time per unit of length, i-th component of which is evaluated by the following formula

$$q_i = q_0 \cdot \frac{\tau_i}{|\bar{\tau}_b|} - C \cdot q_0 \cdot \frac{\partial h}{\partial x_i}, \quad i = 1,\ 2 \tag{6}$$

Here, the first term represents the component of soil particles transport induced by flow in the basin, and the second addend soil shift due to bottom surface irregularities.

The accumulation factor is

$$q_0 = \begin{cases} 12 \cdot \sqrt{g \cdot (s-1) \cdot d^3} \cdot (\theta - \theta_c) \cdot \sqrt{\theta}, & \theta > \theta_c \\ 0, & else \end{cases} \tag{7}$$

the value of soil transport on the horizontal bottom which is equal to zero in case when Shields' parameter does not exceed the critical value of θ_c. Herewith $\theta_c = \theta_0 \frac{\sin(\alpha+\varphi)}{\sin(\varphi)}$, where θ_0 - Shields' rejection number for horizontal bottom, α - tilting angle of bottom, and φ - angle of repose equal to $23°$. In accordance with this formula, Shields rejection number compared with this parameter for horizontal bottom increases while moving up the slope and decreases when moving down. According to calculations, the value θ_0 is in the range of $0,01 < \theta_c < 0,06$.

After receiving the bed load transfer vector for computing the bottom changes formed due to soil transfer, the mass balance equation is solved

$$\frac{\partial h}{\partial t} = \frac{1}{1-\mathrm{p}} \cdot \sum_i \frac{\partial q_i}{\partial x_i}, \quad i = 1,\ 2, \tag{8}$$

written relating to function h of the elevation of the formed bottom profile over its initial level; here p bed load porosity.

4 Results of Numerical and Experimental Studies

The present paper represents several sets of numerical experiments compared with the laboratory tests laid out in [1] in detail.

Numerical Domain (Fig. 1) corresponds to the operating area in a model tank with a gravity type oil platform model. The operating area has the size of 12x6 meters. Left bottom corner is considered to be the origin of coordinates. At a distance of 4 meters from the Inlet there is an oil platform model with the size of 2x2 meters, the model has chamfered corners (45 degrees) with the sides of 0.2x0.2 meters. The depth of fluid in the tank is 0.3 meters.

The patterned finite-volume grid consisting of octagons is used for discretization of a numerical domain. The partition along axes Ox and Oy amounts for
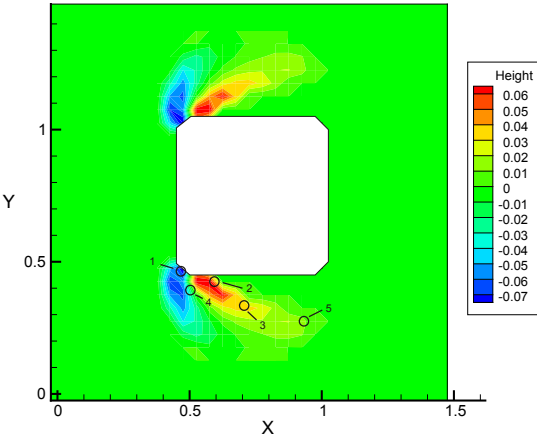
Fig. 2. Structure of soil erosion. Laminar flow model.

20 points per 1 meter, and along axis Oz - 20 points per 0.3 meter with the concentration to the bottom of a numerical domain (proportion of the vertical dimension of a near-bottom mesh to the top one 1:60). The vertical dimension of a near-bottom mesh is 1 mm. Such partition is prescribed by 556 664 points and it contains 531 200 meshes.

The first set of computation refers to the use of a laminar fluid flow model studied in [3] in detail. The velocity of inlet flow corresponds to the average by depth of fluid flow velocity in a laboratory test and is equal to 0.25 m/s. Fig. 2, Fig. 3 contain soil discontinuity structures received in numerical and laboratory studies accordingly.

Number of point	Numerical result, mm	Measurement result, mm
1	-77.75	-75.34
2	74.64	71.81
3	31.39	33.09
4	-34.42	-31.19
5	10.21	11.17

Table 1. Comparison between experimental and numerical studies

The detailed numerical studies of soil erosion undertaken in [3] with the use of finite difference methods and reproduced in this study with the help of finite volume approaches show that in case of low velocity (up to 0.3 m/s) the use of laminar fluid flow model allows to receive good quantitative agreement with laboratory tests data with the significant economy of computational resources.
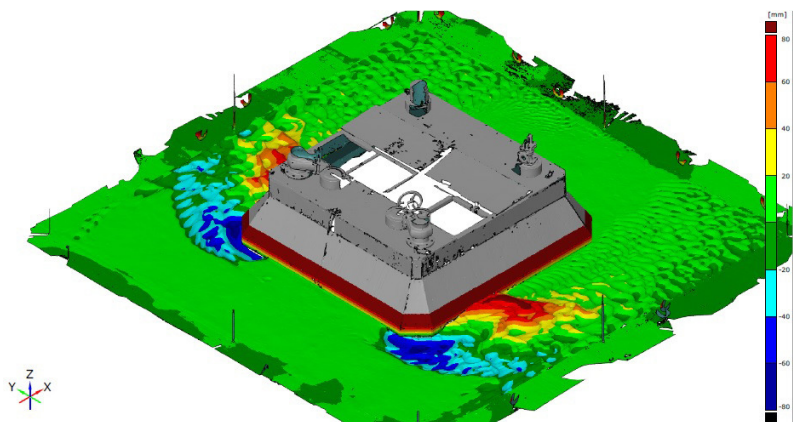
Fig. 3. Structure of soil erosion. Laboratory experiments data (mm).

Table 1 contains the bottom height function value resulted from numeric computation and experiment in the points shown in Fig. 2.

The second set of computation refers to the use of a turbulent fluid flow model represented in this study, with the same value (0.25 m/s) of inlet flow velocity. These computations applied structured computational grid. The segmentation along axes OX and OY is 40 points per 1 meter and along the axis OZ is 40 points per 0.3 meter, with the concentration to the bottom of the computation domain. The vertical dimension of a near-bottom mesh is 0.01 mm which corresponds to dimensionless distance to the wall $y^+ = 1$.

Fig. 4 shows streamlines drawn up in horizontal plane with z=0.1 for different time points demonstrating eddy formation (a), its development (b), separation (c) and cycle mode (d, e). These figures allow suggesting the periodic nature of flow. Though the chart (represented in Fig. 5) of correspondence of velocity vector magnitude to time (0 sec < t < 1000 sec) in the point beside the streamlined platform with the following coordinates (7, 4.5, 0.15) allows to conclude that the flow nature is close to periodic, but it is not such.

Fig. 6 contains space patterns of fluid flow demonstrating formation and development of complex eddies.

Fig. 7 represents the structure of soil erosion received by a numerical experiment.

The results of computation correspond qualitatively and quantitatively with the data of laboratory studies and results of numerical computation received with the use of a laminar fluid flow model.

The third set of computation refers to the increase of inlet fluid flow velocity. Fig. 8 demonstrates the pattern of soil erosion when the inlet flow velocity is equal to 0.5 m/s.
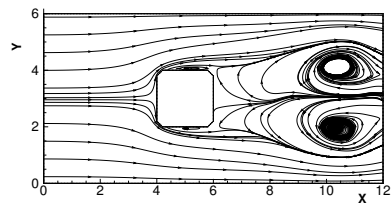
In this case the flow structure acquires significantly turbulent nature that stipulates essentially different arrangement of erosion areas and accretion areas.
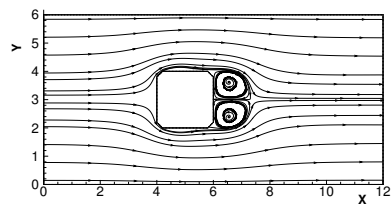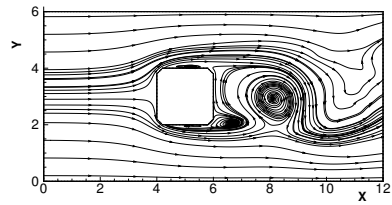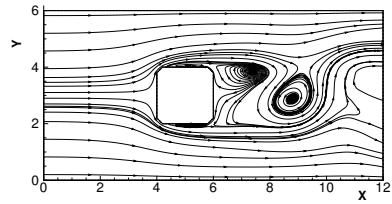
a) t=10 s.
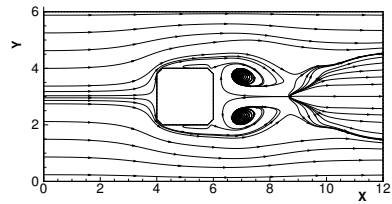
b) t = 30 s.

c) t = 80 s.

d) t = 130 s.

e) t = 140 s.

Fig. 4. Streamlines drawn up in horizontal plane z=10.
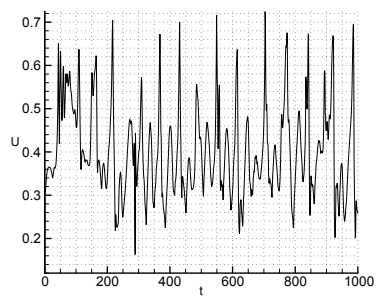
Fig. 5. Flow time variations in the point (7, 4.5, 0.15)
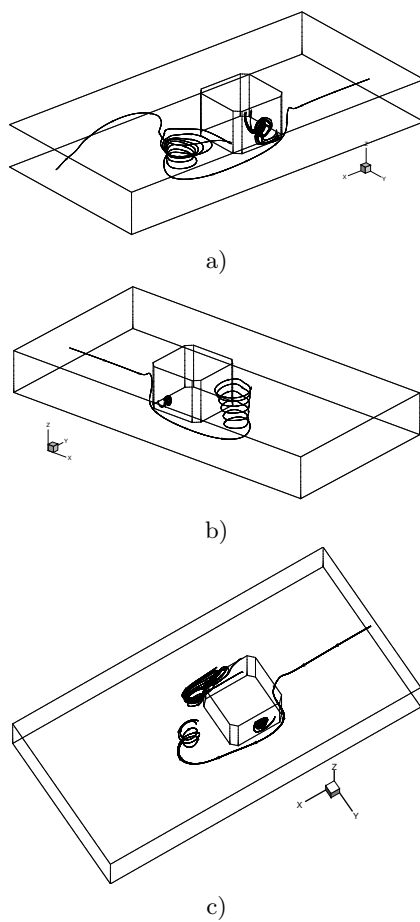

a)

b)

c)

Fig. 6. Formation and development of complex eddies.
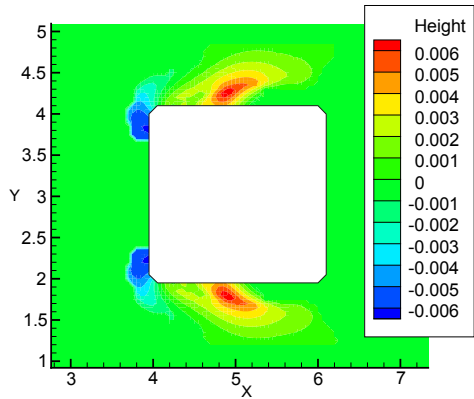
Fig. 7. Structure of soil erosion. Turbulent flow model.
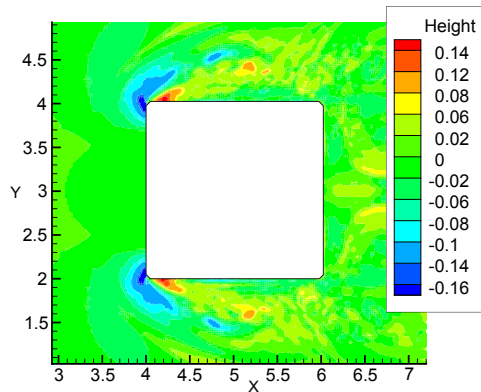

Fig. 8. Structure of soil erosion. Turbulent flow model in case of high velocity.

5   Conclusion

The present paper represents the numerical studies of the process of soil erosion near foundations of gravity type oil platforms under conditions of developing turbulence of fluid flow. The calculation data show that when the flow hydro-dynamic behavior is of low values, the small-scale turbulence has little impact on erosion structure, and in this case the laminar flow model for computing bottom velocity is more preferable. If the input flow velocity is increased, the turbulence mode of fluid flow obtains the paramount importance for outwash

and inwash (accretion) areas, and the application of the turbulent model for estimating hydrodynamic values becomes principal in this case.

References

1. Zakharov, Y.N., Nudner, I.S., Gaydarov, N.A., Ivanov, K.S., Semenov, K.K., Lebedev, V.V., Belyaev N.D., Mishina A.V., Schemelinin L.G.: Numerical and Experimental Studies of Soil Scour Caused by Currents near Foundations of Gravity-Type Platforms. In: International Conference on Civil Engineering, Energy and Environment (CEEE-2014), pp. 190–197. Hong Kong (2014)
2. Zakharov, Y.N., Nudner, I.S., Gaydarov, N.A., Ivanov, K.S., Semenov, K.K., Lebedev, V.V., Mishina A.V., Schemelinin L.G.: Numerical and Experimental Studies of Soil Scour near Foundations of Platforms. In: Advanced technologies of hydroacoustics and hydrophysics, pp. 239–241. SPb (2014)
3. Zakharov, Y.N., Nudner, I.S., Gaydarov, N.A., Ivanov, K.S., Semenov, K.K., Lebedev, V.V., Belyaev N.D., Mishina A.V., Schemelinin L.G.: Impact of waves and currents on the soil near gravity-type offshore platform foundation: numerical and experimental studies. In: Twenty-fifth (2015) International Ocean and Polar Engineering Conference ISOPE-2015, pp. 807–814. Kona, Hawaii, USA (2015)
4. Menter, F. R.: Zonal two equation k turbulence models for aerodynamic flows. In: AIAA 24th Fluid Dynamic Conference. Orlando, Florida (1993)
5. Wilcox D.C.: Formulation of the $k-\omega$ turbulence model revisited. J. AIAA, 46, No. 11, 2823–2838 (2008)
6. Solberg, T., Hjertager, B. H., Bove, S.: CFD modelling of scour around offshore wind turbines in areas with strong currents. Technical report 5, Esbjerg Institute of Technologym Aalborg University (2005)
7. Brørs, B.: Numerical modeling of flow and scour at pipelines. J. Hydraul. Eng. 125, 511–523 (1999)